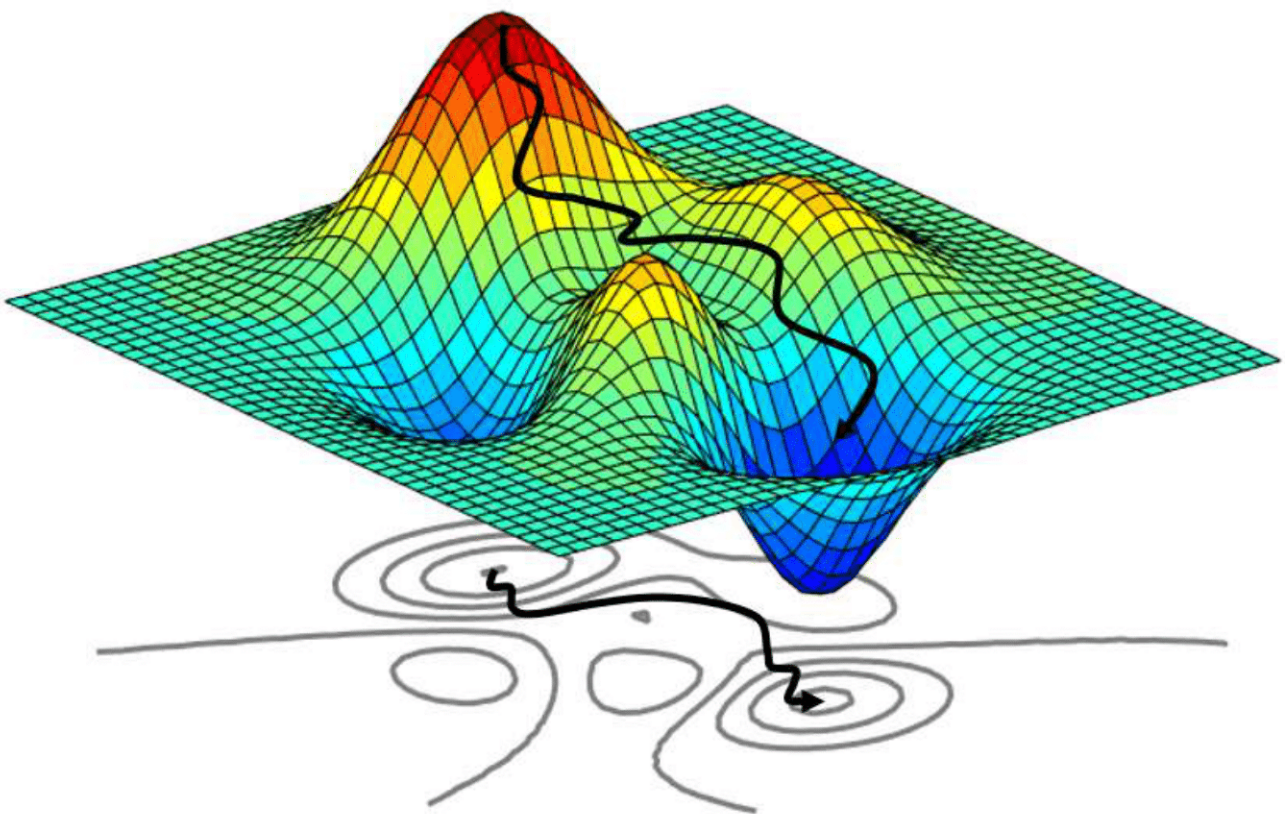


AE4205 - MDO for Aerospace applications

MDO of a wing to minimize mission fuel of the aircraft B767-300

Team 16 - Retake session

Vittorio De Lauso 5833000
Kirsten Coutinho 4778707



AE4205 - MDO for Aerospace applications

MDO of a wing to minimize mission fuel of the
aircraft B767-300

by

Team 16 – Retake session

Vittorio De Lauso	5833000
Kirsten Coutinho	4778707

Part 1

1.1. Part 1.1 - Parameterization and specification of the MDO problem**1.1.1. Nomenclature****Abbreviations**

Abbreviation	Definition
A-W	Aircraft less Wing group
CST	Class Shape function Transformation
EMWET	Elham Modified Weight Estimation Technique
HLD	High Lift Devices
LE	Leading Edge
MDF	Multi Discipline Feasible
MDO	Multi-disciplinary Design Optimization
MTOW	Maximum Take-Off Weight
Q3D	Quasi-Three-Dimensional
TE	Trailing Edge
XDSM	eXtended Design System Matrix
ZFW	Zero Fuel Weight

Symbols

Symbol	Definition	Unit
Λ_{TE_1}	Sweep angle of the trailing edge of the inboard wing segment	[°]
Λ_{TE_2}	Sweep angle of the trailing edge of the outboard wing segment	[°]
α_{WI}	Wing incidence angle	[°]
α_r	Twist angle at the root	[°]
α_k	Twist angle at the kink	[°]
α_t	Twist angle at the tip	[°]
b_k	Spanwise distance of the kink with respect to the fuselage centerline	[m]

Symbol	Definition	Unit
β	Dihedral angle	[°]
c_r	Root chord length	[m]
c_k	Kink chord length	[m]
c_t	Tip chord length	[m]
b	Span of the wing	[m]
t_{rk}	Taper ratio at the kink	[-]
t_{rt}	Taper ratio at the tip	[-]
x_{fs}	Chordwise position of the front spar	[m]
x_{rs}	Chordwise position of the rear spar	[m]
A_{tank}	Cross-sectional area of fuel tank	[m ²]
A_r	Bernstein coefficients for the root airfoil	[-]
A_t	Bernstein coefficients for the tip airfoil	[-]
$A_{r-lower}$	Bernstein coefficients for the root airfoil - lower curve	[-]
$A_{r-upper}$	Bernstein coefficients for the root airfoil - upper curve	[-]
$A_{t-lower}$	Bernstein coefficients for the tip airfoil - lower curve	[-]
$A_{t-upper}$	Bernstein coefficients for the tip airfoil - upper curve	[-]
a_c	Speed of sound at cruise conditions	[$\frac{m}{s}$]
h_c	Altitude at cruise conditions	[m]
M_c	Mach number at cruise conditions	[-]
M_{MO}	Mach number at critical conditions	[-]
$N_{STATIONS-TANK}$	Number of fuel 'tank stations' across span of wing	[-]
V_c	Cruise Velocity	[$\frac{m}{s}$]
V_{tank}	Volume of fuel tank	[m ³]
V_{MO}	Maximum operating velocity	[$\frac{m}{s}$]
μ_c	Dynamic Viscosity at cruise altitude	[$\frac{kg}{ms}$]
Re_c	Reynolds number at cruise conditions	[-]
Re_{MO}	Reynolds number at critical conditions	[-]
R_c	Design Range	[m]
ρ_c	Air Density at cruise altitude	[$\frac{kg}{m^3}$]
n_{max}	Maximum Load factor	[-]

Symbol	Definition	Unit
$n_{section}$	Number of section used to define the wing plan-form	[-]
$n_{airfoil}$	number of wing sections at which airfoils are provided	[-]
n_{engine}	Number of engines installed in each half wing	[-]
C_m	Moment coefficient	[-]
$C_{m_{crit}}$	Critical moment coefficient	[-]
C_L	Lift coefficient	[-]
C_D	Drag coefficient	[-]
$C_{L_{crit}}$	Critical lift coefficient	[-]
W_{TO-max}	Maximum take off weight	[N]
W_{fuel}	Weight of the fuel	[N]
W_{A-W}	Weight of the entire aircraft (design payload included), excluding the weight contributions of fuel and wing structure	[N]
$W_{str-wing}$	Wing structural weight	[N]
W_{des}	Design weight	[N]
L_{des}	Design Lift	[N]
D_{A-W}	Drag generated by the A-W group	[N]
D_{wing}	Drag generated by the wing	[N]
f_{tank}	Factor to account for the wing-tank volume occupied by other elements	[-]
ρ_{fuel}	Aviation fuel density	$[\frac{kg}{m^3}]$
$TSFC$	Thrust specific fuel consumption	$[\frac{N}{Ns}]$
F	Stiffened panel efficiency factor	[-]

Table 1.2: Nomenclature table indicating symbols, their description and units

1.1.2. Parameterization

In the assignment it is requested that the parameterization must be such as to allow modification of: Lifting areas, Sweep angles, Twist angles, Chord lengths and taper ratios.

It is also requested that the following parameters should be assumed constant:

Parameter	Description	Units
Λ_{TE_1}	Trailing edge sweep angle of the inboard wing segment	[°]
b_k	Spanwise distance of the kink with respect to the fuselage centerline	[m]
β	Dihedral angle	[°]
α_{WI}	Wing incidence angle	[°]

Table 1.3: Constant parameters of the parameterization

Wing planform

The wing planform has been parameterized as a composition of two trapezoidal components: an inboard wing segment, whose characteristics have been denoted by the use of the subscript $()_1$ and an outboard wing segment, which has the subscript $()_2$.

In Fig. 1.1 the spanwise distance of the kink is computed with respect to the fuselage – wing intersection. Given that there is no change in the fuselage radius, the spanwise distance of the kink computed with respect to the fuselage – wing intersection and the spanwise distance of the kink computed with respect to the fuselage centerline only differ by a constant.

Airfoils

Two different airfoils have been defined, one at the wing root and one at the wing tip, the airfoil at the kink is defined as a linear interpolation of root and tip airfoils.

The definition of the airfoils has been carried out using the 2D CST Parameterization method, using CST curves of order 5, so 6 Bernstein coefficients for both the upper part and lower part of each airfoil.

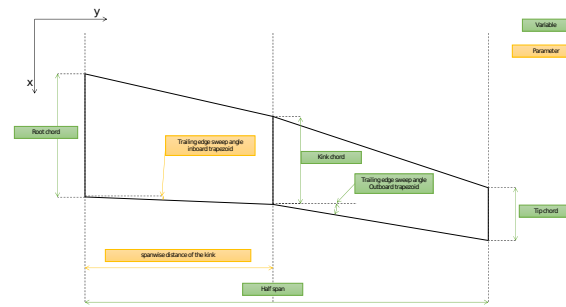


Figure 1.1: Illustration of the adopted parameterization for the wing - Wing planform variables and parameters

Other parameters and variables not visible on the x-y plane

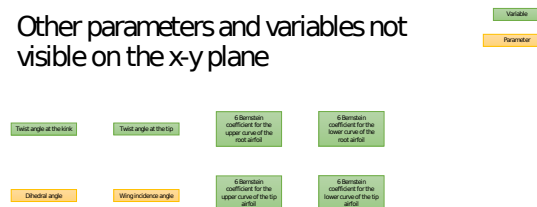


Figure 1.2: Illustration of the adopted parameterization for the wing - Variables and parameters not visible on the wing planform plane

Variable	Description	Units
Λ_{TE_2}	Sweep angle of the trailing edge of the outboard wing segment	[°]
α_k	Twist angle at the kink	[°]
α_t	Twist angle at the tip	[°]
c_r	Root chord length	[m]
c_k	Kink chord length	[m]
c_t	Tip chord length	[m]
b	Span of the wing	[m]
A_r	Bernstein coefficients for the root airfoil	[–]
A_t	Bernstein coefficients for the tip airfoil	[–]

Table 1.4: Variables from the parameterization

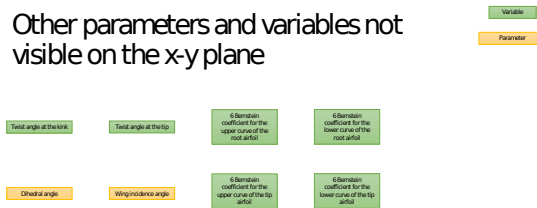


Figure 1.3: Illustration of the adopted parameterization for the tanks

As it can be seen in the figures, the variables considered with this parameterization are listed in table 1.4.

As a general rule, A_r , so the Bernstein coefficients for the root airfoil (same for kink and tip airfoils), is a vector composed of two vectors: $A_{r-lower}$ and $A_{r-upper}$, in this order, respectively Bernstein coefficients for the root airfoil - lower curve and upper curve.

1.1.3. Design vector

The position of the spars has been kept fixed during the optimization, in order to avoid too high computational costs.

The total number of variables in the design vector is 31, of which 7 deal with the planform shape and angles and $24 = 6 \cdot 4$ are the 4 sets of 6 Bernstein coefficients that describe the airfoils.

Variable	Description	Units
Λ_{TE_2}	Sweep angle of the trailing edge of the outboard wing segment	[°]
α_k	Twist angle at the kink	[°]
α_t	Twist angle at the tip	[°]
c_r	Root chord length	[m]
c_k	Kink chord length	[m]
c_t	Tip chord length	[m]
b	Span of the wing	[m]
$A_{r-lower}$	Bernstein coefficients for the root airfoil - lower curve	[−]
$A_{r-upper}$	Bernstein coefficients for the root airfoil - upper curve	[−]
$A_{t-lower}$	Bernstein coefficients for the tip airfoil - lower curve	[−]
$A_{t-upper}$	Bernstein coefficients for the tip airfoil - upper curve	[−]

Table 1.5: Design vector with description of each variable

1.1.4. Initial point and bounds

Given that it has not been possible to find the actual airfoils of the reference aircraft, the Withcomb-135 airfoil has been used: scaled to a thickness ratio of 14% for the wing root section and scaled to 8% for the tip section.

The values of the parameters discussed previously are presented in Table 1.6

Parameter	Value	Units
Λ_{TE_1}	6.3402	[°]
b_k	5.352	[m]
β	5	[°]
α_{WI}	4.25	[°]

Table 1.6: Initial values of the parameters from the parameterization

Other parameters which have been used are the weight of the engine, its position along the wing span and its specific fuel consumption, found in the manufacturer website [1].

Furthermore, the initial point and bounds of the design vector can also be found in Table 1.6.

Variable	Lower bound	Initial point	Upper bound
Λ_{TE_2}	5	19.5367	25
α_k	0	3	4
α_t	0	-1	-2
c_r	7	9.5	13
c_k	4	6.8096	8
c_t	1	1.8785	8
b	40	47.57	60
$A_{r-lower}$	-0.1182	-0.2363	-0.0345
	-0.0857	-0.1713	-0.2570
	-0.0246	-0.0493	-0.0739
	-0.2501	-0.5001	-0.7502
	0.0385	0.0770	0.1155
	0.1706	0.3413	0.5120
$A_{r-upper}$	0.1226	0.2451	0.3677
	0.0417	0.0834	0.1251
	0.1408	0.2815	0.4222
	0.0464	0.0927	0.1391
	0.1463	0.2926	0.4389
	0.1997	0.3994	0.5991
$A_{t-lower}$	-0.0675	-0.1350	-0.2025
	-0.0490	-0.0980	-0.1470
	-0.0140	-0.0280	-0.0420
	-0.1431	-0.2861	-0.4292
	0.0221	0.0442	0.0663
	0.0975	0.1949	0.2924
$A_{t-upper}$	0.0700	0.1400	0.2100
	0.0239	0.0478	0.0717
	0.0803	0.1605	0.2408
	0.0267	0.0534	0.0801
	0.0834	0.1668	0.2502
	0.1142	0.2284	0.3426

Table 1.7: Bounds and initial point of the design vector

For **wing sweep**, an increase in this variable can potentially lead to a decrease in fuel weight. This can occur because an increase in sweep leads to an increase in the effective aspect ratio of the wing due to the reduction in the effective chord of the wing. The increase in aspect ratio leads to reduced the strength of the potential shock waves that may form and contribute to wave drag in the transonic and supersonic regimes. The reduction in drag can lead to a lower amount of fuel required. [2] On the other hand, a wing that is too far swept will perform poorly under loads. The sweep increases the moment arm leading to higher moment and torsion forces. To account for this, the wing must be reinforced which causes an increase in wing structural weight. This will result in more fuel required. Keeping this information in mind, the wing sweep bounds are kept relatively relaxed.[3] Similarly, the **span** and **chords** of the wing should be allowed to vary as it can be beneficial to have a long and slender wing that increases the aspect ratio to reduce drag. However, again this can lead to reinforcement required thus increasing the wing structural weight and as a consequence, the fuel weight.[2] **Twist** in an aircraft is typically used to allow for the wing to maintain a uniform lift distribution along the wing. Not using twist can result in wing tip stall. Maintaining a uniform lift distribution along the wing can result in an improved L/D ratio and therefore a lower fuel weight.

However, similar to the tradeoff for wing sweep, wing twist can also result in an increased structural weight due to reinforcements as the wing experiences increased structural stresses.[4]

The upper and lower bounds for the bernstein coefficients should be quite relaxed. This is because it is expected that the shape of the airfoil along the wing will also be quite influential in the optimization. Therefore, to not discard any potential shapes that could results from the optimization, the bounds are kept relaxed. The upper and lower bounds along with the initial airfoils for the root and tip airfoil have been plotted in Figure 1.4 and Figure 1.5 respectively.

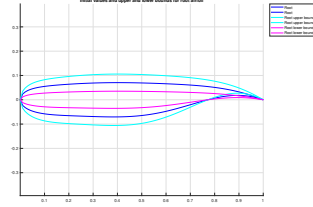


Figure 1.4: Plot showing the initial root airfoil along with the lower and upper bounds

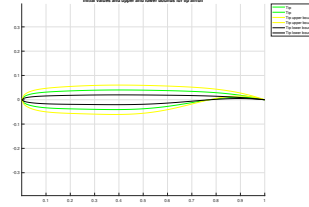


Figure 1.5: Plot showing the initial tip airfoil along with the lower and upper bounds

1.1.5. Objective function

The design point at which the wing is optimized is the mid-cruise condition. The weight of the aircraft at the design point is the following:

$$L_{des}(\bar{x}) = W_{des}(\bar{x}) = \sqrt{W_{TO-max}(\bar{x})[W_{TO-max}(\bar{x}) - W_{fuel}(\bar{x})]} \quad (1.1)$$

The objective function consists in minimizing the fuel mass for the given mission range:

$$R = \frac{V}{C_T} \cdot \frac{L}{D} \cdot \ln \frac{W_{start-cr}}{W_{end-cr}} \quad (1.2)$$

$$W_{fuel} = \left(1 - 0.938 \cdot \frac{W_{end-cr}}{W_{start-cr}}\right) \cdot W_{TO-max} \quad (1.3)$$

1.1.6. Constraints

Inequality constraints:

There are two inequality constraints:

1. Tank Volume inequality constraint:

$$W_{fuel}(\bar{x}, \hat{y}) - \rho_{fuel} V_{tank}(\bar{x}) f_{tank} \leq 0 \quad (1.4)$$

W_{fuel} is computed from the discipline of Performance, which receives in input a consistent set of input and target variables, after their iteration through the MDA block.

V_{tank} is computed from the design vector in the following way:

- Given the chordwise position of front and rear spar, upper and lower curve of the airfoils at root, kink and tip, it is possible to compute an approximated tank volume.
- For a number of $N_{STATIONS-TANK}$, the cross-sectional area of the tank (A_{tank}) is computed at section i , as it can be seen in the Figure 1.6

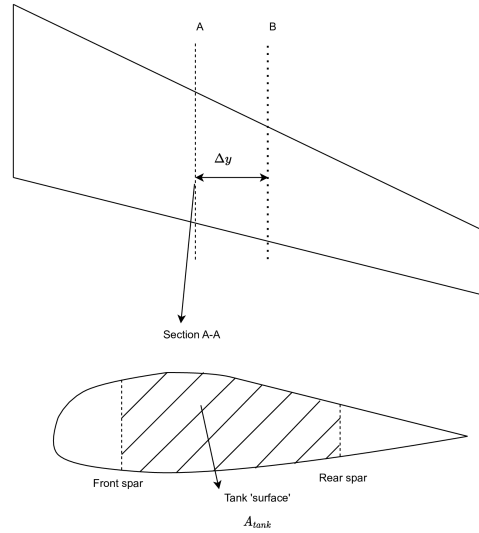


Figure 1.6: Scheme for tank volume calculation

- Then the volume of the entire tank is computed assuming that the cross-sectional area of the tank stays constant in the intervals in which the wing has been divided, considering that the tank in the wing starts at the intersection between root and fuselage and finishes at the tank limit $y_{tank,lim} = 0.85\%$ of the half span. Thus, the tank volume is computed according to:

$$V_{tank} = \sum_{i=1}^{N_{STATIONS-TANK}} A_{tank}(i) \cdot \Delta y(i) \quad (1.5)$$

2. Wing Loading inequality constraint:

$$\frac{W_{TO-max}(\bar{x}, \hat{y})}{S(\bar{x})} - \frac{W_{TO-max}^{(0)}}{S^{(0)}} \leq 0 \quad (1.6)$$

Equality constraints:

There are no equality constraints.

1.1.7. Normalization

The design vector, the initial point, the bounds, the constraints and the objective function have been normalized as follows:

The design vector, the initial design vector (or initial point) and the bounds vector (upper and lower) have been normalized with respect to the initial design vector, while the constraints and the objective function have been normalized with respect to their value computed with the initial design vector. Normalizing the design vector ensures that the solver will not suffer from high gradients for large variable changes when computing the objective function.

Normalized design vector: It is shown in the table; the description of the single variables can be retrieved, in a dimensional form, in Tab. 1.5:

Variable
$\frac{\Lambda_{TE2}}{\Lambda_{TE2}^0}$
$\frac{\alpha_k}{\alpha_k^0}$
$\frac{\alpha_t}{\alpha_t^0}$
$\frac{c_r}{c_r^0}$
$\frac{c_k}{c_k^0}$
$\frac{c_t}{c_t^0}$
$\frac{b}{b^0}$
$\frac{A_{r-lower}}{A_{r-lower}^0}$
$\frac{A_{r-upper}}{A_{r-upper}^0}$
$\frac{A_{t-lower}}{A_{t-lower}^0}$
$\frac{A_{t-upper}}{A_{t-upper}^0}$

Table 1.8: Normalized design vector

Normalized initial point and bounds: The initial point has been normalized with respect to itself, so it will result in an array of 31 ones. The bounds are shown in table 1.9

Normalized constraints They are the following:

Tank Volume inequality constraint:

$$\frac{W_{fuel}(\bar{x})}{\rho_{fuel} V_{tank}(\bar{x}) f_{tank}} - 1 \leq 0 \quad (1.7)$$

Wing Loading inequality constraint:

$$\frac{\frac{W_{TO-max}(\bar{x})}{S(\bar{x})}}{\frac{W_{TO-max}^{(0)}}{S^{(0)}}} - 1 \leq 0 \quad (1.8)$$

Normalized objective function The function that has to be minimized is:

$$\frac{W_{fuel}(\bar{x})}{W_{fuel}(x^0, y^0)} \quad (1.9)$$

1.1.8. Mathematical notation

$$\underset{\bar{x}}{\text{minimize}} \quad \frac{W_{fuel}(\bar{x})}{W_{fuel}(x^0)} \quad (1.10a)$$

subject to

$$\frac{W_{fuel}(\bar{x})}{\rho_{fuel} V_{tank}(\bar{x}) f_{tank}} - 1 \leq 0, \quad (1.10b)$$

$$\frac{\frac{W_{TO-max}(\bar{x})}{S(\bar{x})}}{\frac{W_{TO-max}^{(0)}}{S^{(0)}}} - 1 \leq 0 \quad (1.10c)$$

Variable	Lower bound	Initial point	Upper bound
$\frac{\Lambda_{TE2}}{\Lambda_{TE2}^0}$	0.2559	1	1.2796
$\frac{\alpha_k}{\alpha_k^0}$	0.0000	1	1.333
$\frac{\alpha_t}{\alpha_t^0}$	0.0000	1	2
$\frac{c_r}{c_r^0}$	0.7368	1	1.3684
$\frac{c_k}{c_k^0}$	0.5874	1	1.1748
$\frac{c_t}{c_t^0}$	0.5323	1	4.2587
$\frac{b}{b^0}$	0.8409	1	1.2613
$\frac{A_{r-lower}}{A_{r-lower}^0}$	0.5000	1	1.5000
	0.5000	1	1.5000
	0.5000	1	1.5000
	0.5000	1	1.5000
	0.5000	1	1.5000
	0.5000	1	1.5000
$\frac{A_{r-upper}}{A_{r-upper}^0}$	0.5000	1	1.5000
	0.5000	1	1.5000
	0.5000	1	1.5000
	0.5000	1	1.5000
	0.5000	1	1.5000
	0.5000	1	1.5000
$\frac{A_{t-lower}}{A_{t-lower}^0}$	0.5000	1	1.5000
	0.5000	1	1.5000
	0.5000	1	1.5000
	0.5000	1	1.5000
	0.5000	1	1.5000
	0.5000	1	1.5000
$\frac{A_{t-upper}}{A_{t-upper}^0}$	0.5000	1	1.5000
	0.5000	1	1.5000
	0.5000	1	1.5000
	0.5000	1	1.5000
	0.5000	1	1.5000
	0.5000	1	1.5000

Table 1.9: Normalized lower bounds, initial point and upper bounds

1.2. Part 1.2 - XDSM

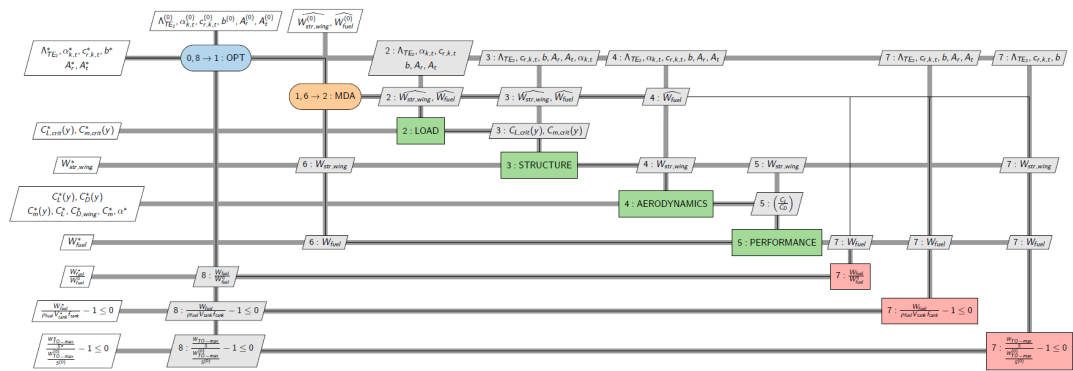


Figure 1.7: *XDSM*

2

Part 2

2.1. Settings and results

2.1.1. Settings

Option	Value/ Setting
Display	iter-detailed
Algorithm	sqp
FunValCheck	off (default)
DiffMinChange	1×10^{-2}
DiffMaxChange	5×10^{-1}
ConstraintTolerance	1×10^{-4}
OptimalityTolerance	1×10^{-6} (default)
StepTolerance	1×10^{-6} (default)
FunDiffType	forward (default)
Time needed to converge to optimum	8.62484×10^3 [s]
Number of required iterations	8
Number of objective function evaluations	137
Average time required per iteration	1078.1 [s]
Achieved first order optimality	0.904343
Max constrainT violation	0

Table 2.1: Options and criteria assigned to the *fmincon* function as well as results of the optimization

The MATLAB termination message resulting from the optimization process is presented below:

```
'Local minimum possible. Constraints satisfied.

fmincon stopped because the size of the current step is less than
the value of the step size tolerance and constraints are
satisfied to within the value of the constraint tolerance.

<stopping criteria details>

Optimization stopped because the relative changes in all elements of x are
less than options.StepTolerance = 1.000000e-06, and the relative maximum constraint
violation, 0.000000e+00, is less than options.ConstraintTolerance = 1.000000e-04.'
```

Figure 2.1: Output message from the optimization process

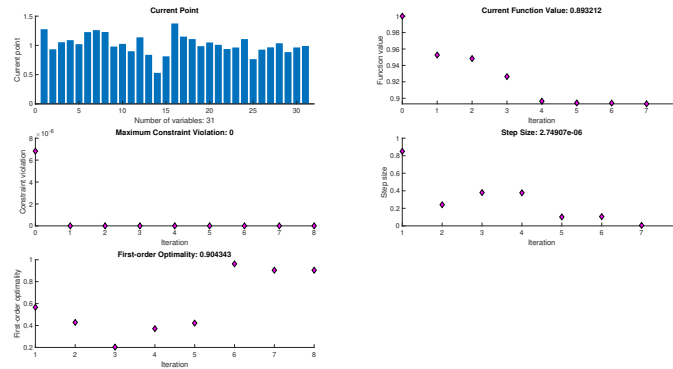


Figure 2.2: Optimization plots with plot of the convergence history of the objective function

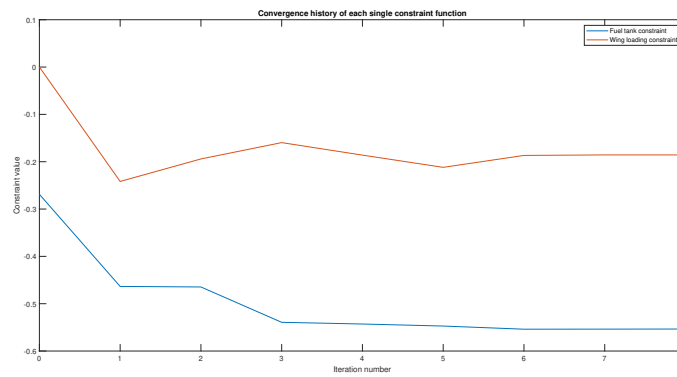


Figure 2.3: Convergence history of each single constraint

2.2. Results

Having implemented the optimization algorithm to the problem, the following results were obtained. They have been presented in Table 2.2 along with the initial values of the design vector(not normalized).

Variable	Initial	Final	Units
W_{fuel}	35123.8	31407.9	kg
Λ_{TE_2}	19.5367	24.9404	deg
α_k	3	2.79932	deg
α_t	-1	-1.05396	deg
c_r	9.5000	10.3473	m
c_k	6.81096	6.95043	m
c_t	1.8785	2.30468	m
b	47.57	60	m
$A_{lower_{root}}$	-0.2363	-0.290338	—
	-0.1713	-0.16789	—
	-0.0493	-0.0505758	—
	-0.5001	-0.450008	—
	0.0770	0.0875877	—
	0.3413	0.286012	—
$A_{upper_{root}}$	0.2451	0.129975	—
	0.0834	0.0677433	—
	0.2815	0.386922	—
	0.0927	0.106653	—
	0.2926	0.324136	—
	0.3994	0.39419	—
$A_{lower_{tip}}$	-0.1350	-0.141685	—
	-0.0980	-0.098882	—
	-0.0280	-0.0262503	—
	-0.2861	-0.275694	—
	0.0442	0.0489786	—
	0.1949	0.149054	—
$A_{upper_{tip}}$	0.1400	0.129824	—
	0.0478	0.0461557	—
	0.1605	0.166302	—
	0.0534	0.0472549	—
	0.1668	0.160932	—
	0.2284	0.226094	—
Constraint 1	-0.2689	-0.5535	-
Constraint 2	3.492e-05	-0.185631	-
$W_{TO_{max}}$	156493	165178	kg
$W_{str_{wing}}$	25387.1	37787.2	kg
V_{fuel}	42.9834	38.4358	m^3
V_{tank}	63.216	92.5689	m^3
C_L	0.6197	0.51568	-
α	-6.21886	-6.69337	deg
$C_{D,wing}$	0.0249938	0.013964	-
$C_{Di,wing}$	0.00737857	0.00298571	-
$\frac{C_L}{C_D}$	15	19.419	-
D_{A-W}	35603.4	35603.4	N
$C_{D,A-W}$	0.0163195	0.0125914	-
W_{A-W}	95982	95982	kg
S	247.433	320.694	m^2
$\frac{W_{TO_{max}}}{S}$	632.468	515.062	kg/m^2
Λ_{TE_1}	6.3402	6.3402	deg
b_k	5.35163	5.35163	m
b_t	18.4334	24.6484	m
AR	9.14553	11.2256	-

Table 2.2: Design vector comparison

2.2.1. Plots

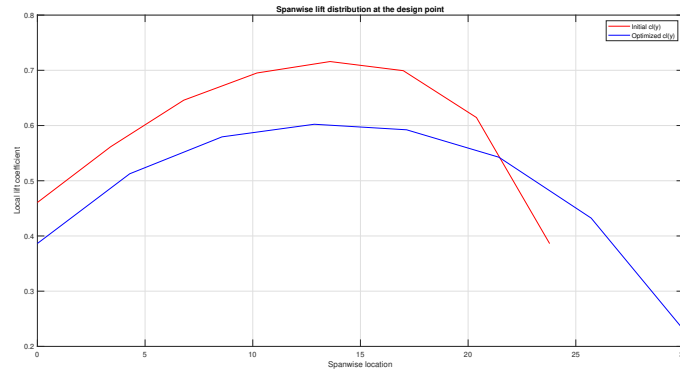


Figure 2.4: Spanwise lift distribution at design point:

Initial wing: Load factor = 1; Weight = 137817.0276 kg ; Flight conditions = 236.0339m/s at 11887.2 m and Reynolds number 26926873.8061

Optimized wing: Load factor = 1; Weight = 148648.2558 kg ; Flight conditions = 236.0339 m/s at 11887.2 m and Reynolds number 28074613.4611

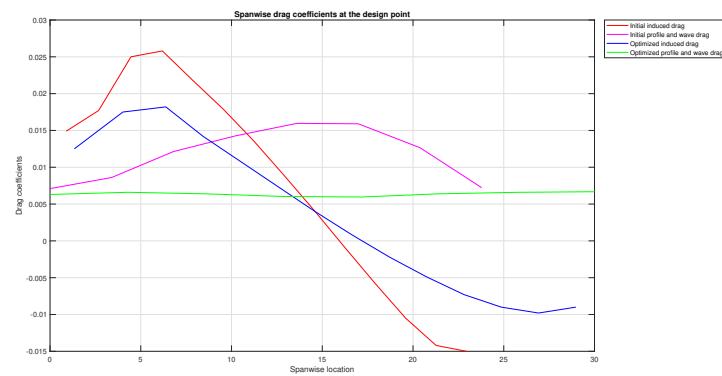


Figure 2.5: Spanwise drag coefficients(induced drag and wave drag) at design point:

Initial wing: Load factor = 1; Weight = 137817.0276 kg ; Flight conditions = 236.0339m/s at 11887.2 m and Reynolds number 26926873.8061

Optimized wing: Load factor = 1; Weight = 148646.3461 kg ; Flight conditions = 236.0339 m/s at 11887.2 m and Reynolds number 28074613.4611

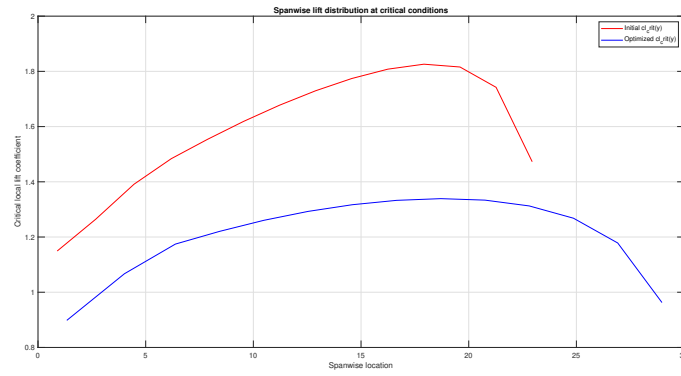


Figure 2.6: Spanwise lift distribution at critical conditions;

Initial wing: Load factor = 2.5; Weight = 156493.3981 kg ; Flight conditions = 253.7364m/s at 11887.2 m and Reynolds number 28946389.3416

Optimized wing: Load factor = 2.5; Weight = 165177.5006 kg ; Flight conditions = 253.7364 m/s at 11887.2 m and Reynolds number 30180209.4707

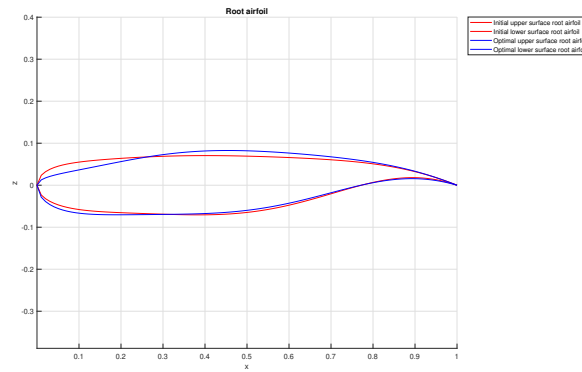


Figure 2.7: Overlapped plots of root airfoils(initial and final)

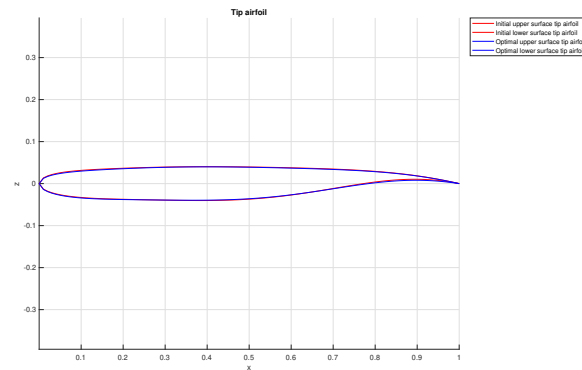


Figure 2.8: Overlapped plots of tip airfoils(initial and final)

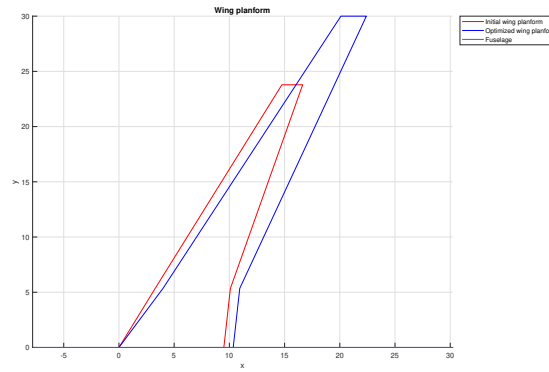


Figure 2.9: Overlapped plots of the initial and optimized wing planform

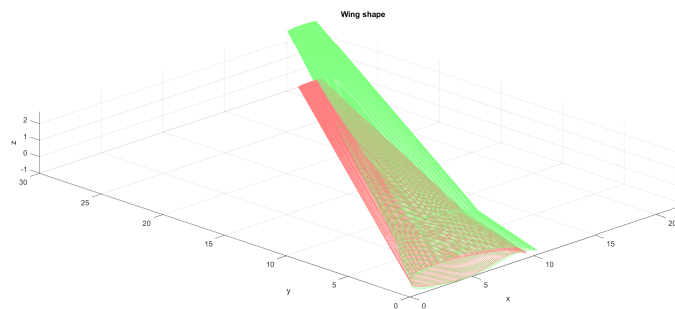


Figure 2.10: Overlapped plots, in isometric view, of the initial (red) and optimized (green) wing shape

2.2.2. Conclusions and critical reflection

The optimization did converge to an optimum. This can be verified from the optimizer message presented in Figure 2.1. Given a sufficiently low step size tolerance, the relative changes in all elements of the design vector at the last iteration were lower. There were also no constraint violations at the end of the optimization, guaranteeing the feasibility of the design, while the MDA guarantees the consistency of the design, which means that certain discipline outputs, used to compute discipline inputs, result in a consistent set, they differ of a negligible amount (specifically, 1×10^{-4}). However, the feasibility and the succeeding of the solver is not a guarantee that the optimum has been found, as explained also in [5]: one way to check if the minimum is, in fact, a local minimum, is to:

1. Change the initial point
2. Check nearby points

Both ways can be checked with one trick, which is to restart the optimization from the optimized point: doing this, the initial point has been changed (even though we are still checking in the same basin of attraction) and the nearby points are checked, with the gradient evaluation at the optimization point.

Using `fmincon`, it is not possible to find the global optimum: in order to do that, it will be necessary to use heuristic algorithms, like surrogate or ga.

The first order optimality, which is a measure of how close a point x is to optimal, is a necessary condition for a point to be optimum, therefore, the fact that its value around the optimum is around 0.9

can make us doubt about the local optimality of the point reached. However, for the feasible and consistent result achieved ($\frac{f_{obj}}{f_{obj}^0} = 89.3\%$), the optimized point represents a satisfactory optimization, even though this value of first order optimality highlights the presence of a gradient of the objective function, possibly in the *direction* of the variables Λ_{TE_2} and b , whose optimum value is positioned on the upper bound.

It could be possible to state that, increasing the upper bound, the solver could have converged to a *better optimum*, but taking into account the absolute, and not relative value of the wingspan, it would be bigger than 60m, which is roughly the same wingspan of the B-747, and given the latest trend in aircraft design to avoid wake vortex encounter [6], it has been our prerogative to limit the dimensions of the aircraft.

Moreover, extending the upper bound of the wingspan makes the Q3DSolver crash, stopping the optimization, therefore the choice has been made also taking into account the limits of the aerodynamics discipline solver, limited for high C_L at such high cruise speeds.

Among the design variables, some of the largest variations were in c_t , b and the shape of the root airfoil (from bernstein coefficients). These changes were expected as the fuel tank holding the fuel is situated within the wing. Therefore, it was most likely that the shape of the wing where most of the fuel could be stored (towards the root) would expand in thickness, while some parts of the airfoil section where the fuel was not contained (the parts between leading edge and front spar and between rear spar and trailing edge) were decreasing in thickness. The shape of the tip airfoil did not vary as much, this could be because not much fuel can be stored towards the tip and therefore, the shape of the airfoil in that location doesn't need to change much.

The aerodynamic performance $\frac{C_L}{C_D}$ increase observed from the initial design was relatively large, with an increase of nearly 30%. The optimization also optimized the wing by increasing the span and sweep, thereby making the wing more slender and increasing the aspect ratio. This could be one of the major contributors to the increase in performance. As explained before, increasing the aspect ratio leads to a decrease in drag and therefore a decrease in thrust required which correlates to an increase in $\frac{C_L}{C_D}$ and a decrease in fuel weight.

It is interesting to note that the maximum takeoff weight, in fact, increased, but the wing surface increased more, bringing the maximum wing loading within the feasible configuration field, with an 18% margin.

The fuel volume constraint, on the other hand, given the strict relation that it has with the objective function, decreased well within the margins for feasibility, resulting in 55% margin.

Both inequality constraints are inactive as their values are negative for the final optimized design (refer to Table 2.2).

The bounds were active for the variables: Λ_{TE_2} , b . It can be seen in the following figure:

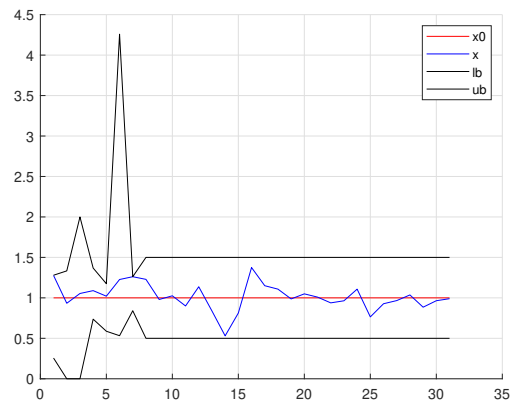


Figure 2.11: Initial and optimized design vectors between lower and upper bounds

However, the other variables of the design stayed within the bounds and did not seem to approach these limits.

Bibliography

- [1] General Electric - Aviation, "Ge - aviation: Cf6."
- [2] W. Phillips, D. F. Hunsaker, and R. Niewoehner, "Estimating the subsonic aerodynamic center and moment components for swept wings," *Journal of aircraft*, vol. 45, no. 3, pp. 1033–1043, 2008.
- [3] Aeronautics Guide, "Homeaerodynamics effect of wing planform - aerodynamics of flight," 2022.
- [4] B.Wainfan, "Design process: Twist effects," 2020.
- [5] The Mathworks, Inc., "fmincon - find minimum of constrained nonlinear multivariable function."
- [6] Skybrary, "En-route wake vortex hazard."